Обзор ArXiv/astro-ph, 04-14 сентября 2023

От Сильченко О.К.

ArXiv: 2309.02492

Massive Optically Dark Galaxies Unveiled by JWST Challenge Galaxy Formation Models

M. Xiao[1✉], P. A. Oesch[1,2], D. Elbaz[3], L. Bing[4], E. Nelson[5], A. Weibel[1], R. P. Naidu[6], E. Daddi[3], R. J. Bouwens[7], J. Matthee[8], S. Wuyts[9], J. Chisholm[10], G. Brammer[2], M. Dickinson[11], B. Magnelli[3], L. Leroy[3], P. van Dokkum[12], D. Schaerer[1], T. Herard-Demanche[7], L. Barrufet[1], R. M. Endsley[10], Y. Fudamoto[13,14], C. Gómez-Guijarro[3], R. Gottumukkala[1], G. D. Illingworth[15], I. Labbe[16], D. Magee[15], D. Marchesini[17], M. Maseda[18], Y. Qin[19,20], N. Reddy[21], A. Shapley[22], I. Shivaei[23], M. Shuntov[2], M. Stefanon[24,25], K. Whitaker[26,2], J. S. B. Wyithe[19,20].

JWST: Безщелевые спектры на площадке GOODS

Here, we exploit the unprecedented imaging and spectroscopic data provided by the JWST FRESCO NIRCam/grism survey[22]. Unlike slit spectroscopy, which can only target pre-selected sources, grism spectroscopy can effectively provide a complete sample of emission line galaxies, with the FRESCO survey reaching down to $\sim 2 \times 10^{-18}$ergs^{-1}cm^{-2} (5σ depth) over a continuous region of 2×62 arcmin^2 in the GOODS-South and North fields[23]. This unique advantage of grism spectroscopy can help to explore missed galaxy populations, e.g., optically dark galaxies. With the deep 4-5μm grism spectra in the F444W filter, we probe Hα+[NII] emission lines at $z = 4.86 - 6.69$ and [OIII]$\lambda\lambda$4960, 5008+Hβ at $z = 6.69 - 9.08$. The FRESCO survey also provides high-resolution NIRCam images (F182M, F210M, and F444W; typical 5σ depth of ~28.2 mag), that complement ancillary data from both HST[24] and now also JWST/JADES[25].

tant, but also the highly dusty and hidden Universe. Based on the deep JWST observations, we find that the three galaxies have extremely red properties (F182M − F444W > 3.5 mag; Fig. 1, Extended Data Fig. 1), due to their significant dust attenuation ($A_V > 3$ mag). Self-consistently, we find that they also have highly dust-obscured star formation rates (SFR_{IR}), which are obtained from far-infrared SED fits with CIGALE, specifically $625 \pm 31 M_\odot$ yr^{-1} for S1, 1030^{+190}_{-150} M$_\odot$ yr^{-1} for S2, and 1137 ± 31 M$_\odot$ yr^{-1} for S3 (see Methods). This indicates that they are in the process of very efficient stellar mass build-up. We find no signs of a significant contribution to the rest-frame optical light by an AGN based on our investigation of the emission lines, source morphology, and multi-wavelength data. Therefore, we conclude that the ultra-massive nature of these three galaxies is reliable.

Нашли 36 далеких объектов

Extended Data

Extended Data Table 1: **Physical properties of the whole sample of optically dark/faint galaxies in FRESCO-S&N fields at $z_{spec} \geq 5$.** (1) IDs; (2) Source ID in FRESCO; (3)(4) Right ascension and declination (J2000) of sources from JWST; (5) Spectroscopic redshift identified from Hα (z_{spec} = 4.86 - 6.69) or [OIII] (z_{spec} = 6.69 - 9.08) emission lines. For sources with only one emission line detected at $> 8\sigma$ (flagged with a "*" exponent), their z_{spec} must be within the 16-84th percentile uncertainties of the z_{phot}; (6) signal-to-noise ratio (S/N) of Hα or [OIII] line; (7)(8)(9) $M_\star$, SFR, and A_V derived from UV-to-NIR SED fitting at a fixed z_{spec} assuming a constant SFH and a Chabrier IMF[28]; (10) AGN candidates, showing broad Hα emission lines ($v_{FWHM,H\alpha,broad} > 1000$ km s^{-1}) with a "little red dot (LRD)" morphology[11]; (11) Source IDs in other work.

S.No.	ID	RA (deg)	DEC (deg)	z_{spec}	S/N$_{H\alpha \text{ or } [OIII]}$	$\log(M_\star)$ $\log(M_\odot)$	log(SFR) $\log(M_\odot \mathrm{yr}^{-1})$	A_V (mag)	AGN	other ID
(1)	(2)	(3)	(4)	(5)	(6)	(7)	(8)	(9)	(10)	(11)
	S-15496	03:32:24.66	-27:44:40.08	5.049*	17.2	$9.72^{+0.12}_{-0.12}$	$1.05^{+0.22}_{-0.16}$	$1.7^{+0.3}_{-0.2}$		
	S-11579	03:32:20.82	-27:47:14.76	5.330*	20.9	$9.44^{+0.11}_{-0.15}$	$0.82^{+0.19}_{-0.14}$	$1.4^{+0.3}_{-0.2}$		
	S-4166	03:32:35.44	-27:50:31.38	5.402*	19.6	$9.14^{+0.08}_{-0.09}$	$0.42^{+0.11}_{-0.08}$	$0.2^{+0.1}_{-0.1}$		
	S-10944	03:32:27.46	-27:47:31.63	5.445	9.14	$8.64^{+0.15}_{-0.15}$	$0.41^{+0.14}_{-0.15}$	$0.3^{+0.2}_{-0.2}$		JADES-116930[79]
	S-11150	03:32:33.26	-27:47:24.91	5.483	30.4	$9.96^{+0.05}_{-0.06}$	$1.17^{+0.06}_{-0.05}$	$1.0^{+0.1}_{-0.1}$		JADES-204851[79]
S1	S-18258	03:32:28.91	-27:44:31.53	5.579*	14.3	$11.37^{+0.11}_{-0.13}$	$2.81^{+0.24}_{-0.16}$	$3.2^{+0.3}_{-0.2}$		OFG28[3], A2GS33[37], ID68[58], ID20[80]
	S-5661	03:32:20.87	-27:49:54.85	5.774*	10.6	$9.56^{+0.12}_{-0.12}$	$1.00^{+0.22}_{-0.14}$	$1.4^{+0.5}_{-0.2}$		
	S-12686	03:32:34.63	-27:46:47.48	6.090*	15.5	$8.29^{+0.15}_{-0.13}$	$0.33^{+0.11}_{-0.14}$	$1.0^{+0.2}_{-0.2}$		
	S-19392	03:32:38.73	-27:44:15.60	6.815	20.9	$9.97^{+0.06}_{-0.07}$	$1.30^{+0.08}_{-0.07}$	$1.1^{+0.1}_{-0.1}$		JADES-219000[79]
	S-6209	03:32:32.12	-27:49:41.72	7.664	8.3	$10.48^{+0.18}_{-0.17}$	$2.05^{+0.22}_{-0.20}$	$3.7^{+0.4}_{-0.4}$		JADES-90354[79]
	S-8010	03:32:20.99	-27:48:53.71	7.846	26.8	$9.30^{+0.12}_{-0.14}$	$0.88^{+0.17}_{-0.12}$	$0.3^{+0.2}_{-0.1}$		JADES-GS-53.08745-27.81492[81]
	N-1002	12:36:35.50	+62:11:04.29	5.050*	10.9	$9.37^{+0.13}_{-0.17}$	$0.82^{+0.27}_{-0.17}$	$1.4^{+0.4}_{-0.3}$		
	N-15498	12:37:08.53	+62:16:50.82	5.086	17.0	$10.12^{+0.11}_{-0.13}$	$1.37^{+0.15}_{-0.14}$	$2.0^{+0.2}_{-0.2}$	LRD	
	N-6079	12:36:55.73	+62:13:36.33	5.093*	15.1	$8.98^{+0.08}_{-0.11}$	$0.27^{+0.13}_{-0.10}$	$0.6^{+0.1}_{-0.1}$		
	N-14409	12:36:17.30	+62:16:24.35	5.146	30.6	$9.09^{+0.09}_{-0.09}$	$0.33^{+0.08}_{-0.09}$	$0.2^{+0.1}_{-0.1}$	LRD	
	N-1257	12:36:24.68	+62:11:17.01	5.167	21.8	$10.04^{+0.14}_{-0.19}$	$1.82^{+0.14}_{-0.16}$	$1.6^{+0.2}_{-0.2}$		
S3	N-2663	12:36:56.56	+62:12:07.37	5.179	22.6	$11.04^{+0.17}_{-0.18}$	$2.48^{+0.29}_{-0.20}$	$3.4^{+0.6}_{-0.4}$		
	N-3188	12:36:51.97	+62:12:26.04	5.187	15.7	$10.58^{+0.14}_{-0.17}$	$2.30^{+0.18}_{-0.17}$	$1.8^{+0.2}_{-0.2}$		HDF850.1[1,82]
	N-7162	12:37:16.90	+62:14:00.90	5.189	21.7	$10.32^{+0.11}_{-0.14}$	$1.71^{+0.15}_{-0.12}$	$1.6^{+0.2}_{-0.1}$		
	N-16116	12:36:56.62	+62:17:07.97	5.194*	14.6	$9.27^{+0.09}_{-0.08}$	$0.51^{+0.09}_{-0.08}$	$0.5^{+0.1}_{-0.1}$		
	N-4014	12:37:12.03	+62:12:43.36	5.221	34.1	$9.76^{+0.09}_{-0.10}$	$1.05^{+0.09}_{-0.11}$	$1.2^{+0.1}_{-0.1}$	LRD	
	N-12839	12:37:22.63	+62:15:48.11	5.240	40.2	$9.94^{+0.08}_{-0.09}$	$1.16^{+0.08}_{-0.08}$	$1.0^{+0.1}_{-0.1}$	LRD	
	N-13733	12:36:13.70	+62:16:08.18	5.243	25.0	$9.54^{+0.09}_{-0.11}$	$0.77^{+0.12}_{-0.11}$	$1.0^{+0.2}_{-0.2}$	LRD	
S2	N-7496	12:36:33.42	+62:14:08.57	5.306	14.3	$11.18^{+0.23}_{-0.17}$	$2.58^{+0.30}_{-0.18}$	$3.4^{+0.8}_{-0.5}$		GN10[29]
	N-16813	12:36:43.03	+62:17:33.12	5.359	48.5	$9.38^{+0.07}_{-0.11}$	$0.67^{+0.05}_{-0.03}$	$0.1^{+0.1}_{-0.0}$	LRD	
	N-9771	12:37:07.44	+62:14:50.31	5.535	101.9	$10.24^{+0.20}_{-0.19}$	$2.05^{+0.12}_{-0.15}$	$1.8^{+0.2}_{-0.2}$	LRD	
	N-6924	12:37:02.72	+62:13:55.07	5.535*	20.3	$9.38^{+0.07}_{-0.08}$	$0.64^{+0.08}_{-0.08}$	$0.3^{+0.1}_{-0.1}$		
	N-14178	12:36:41.69	+62:16:18.39	5.569*	14.7	$8.90^{+0.30}_{-0.25}$	$0.35^{+0.37}_{-0.29}$	$1.2^{+0.9}_{-0.5}$		
	N-1459	12:36:41.95	+62:11:24.47	6.024*	15.7	$9.46^{+0.07}_{-0.09}$	$0.78^{+0.09}_{-0.08}$	$0.4^{+0.1}_{-0.1}$		
	N-12207	12:36:36.47	+62:15:34.72	6.760*	23.5	$9.75^{+0.09}_{-0.11}$	$1.11^{+0.11}_{-0.09}$	$0.6^{+0.1}_{-0.1}$		
	N-9094	12:36:04.62	+62:14:36.71	7.038	73.7	$10.48^{+0.11}_{-0.12}$	$1.91^{+0.15}_{-0.12}$	$1.3^{+0.2}_{-0.1}$		
	N-489	12:36:47.52	+62:10:37.27	7.131	31.4	$9.16^{+0.15}_{-0.19}$	$0.80^{+0.24}_{-0.20}$	$0.7^{+0.3}_{-0.3}$		
	N-8697	12:37:00.04	+62:14:29.00	7.146	19.3	$9.17^{+0.12}_{-0.13}$	$0.69^{+0.17}_{-0.15}$	$0.4^{+0.2}_{-0.2}$		
	N-2756	12:36:20.04	+62:12:09.29	7.190	18.4	$10.00^{+0.08}_{-0.10}$	$1.42^{+0.11}_{-0.11}$	$0.8^{+0.1}_{-0.1}$		
	N-11316	12:36:10.84	+62:15:16.32	7.403*	14.2	$9.55^{+0.11}_{-0.14}$	$1.09^{+0.20}_{-0.16}$	$0.8^{+0.3}_{-0.2}$		
	N-4380	12:36:41.09	+62:12:53.12	8.613	16.4	$9.54^{+0.16}_{-0.15}$	$1.14^{+0.21}_{-0.16}$	$1.0^{+0.3}_{-0.2}$		JADES-GN-189.17121+62.21476[81]

… среди них три ОЧЕНЬ массивные

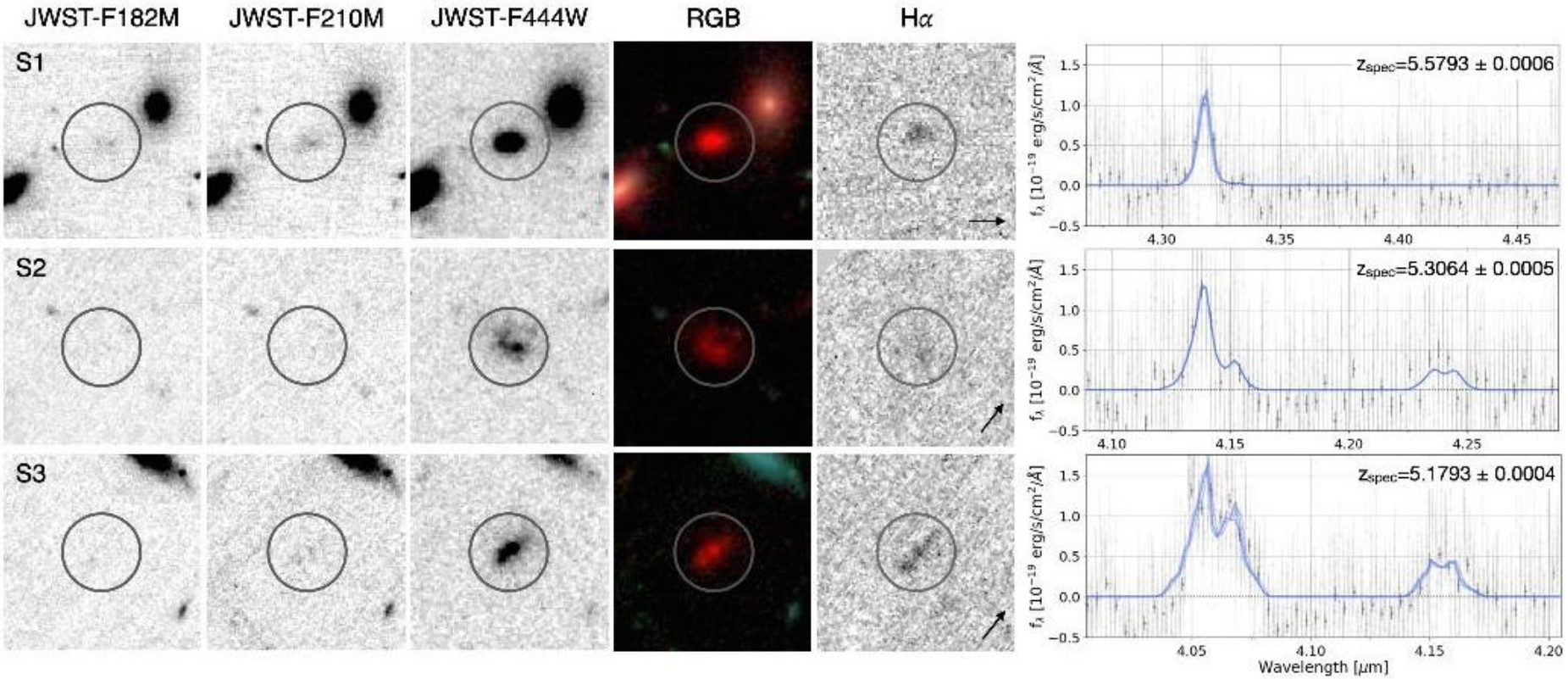

Figure 1: **Images and Spectra of the three optically dark, ultra-massive galaxies from the JWST FRESCO survey.** From left to right: $4'' \times 4''$ stamps obtained in JWST/NIRCam filters (1.82μm, 2.10μm, and 4.44μm), RGB images (F182M in blue, F210M in green, and F444W in red), Hα line map, and 1D spectra (covering Hα, [NII], and [SII] emission lines) obtained from NIRCam/grism observations with the F444W filter. The black arrow in the lower-right corner of Hα line map shows the dispersion direction of the F444W grism.

LCDM-предсказания промахиваются

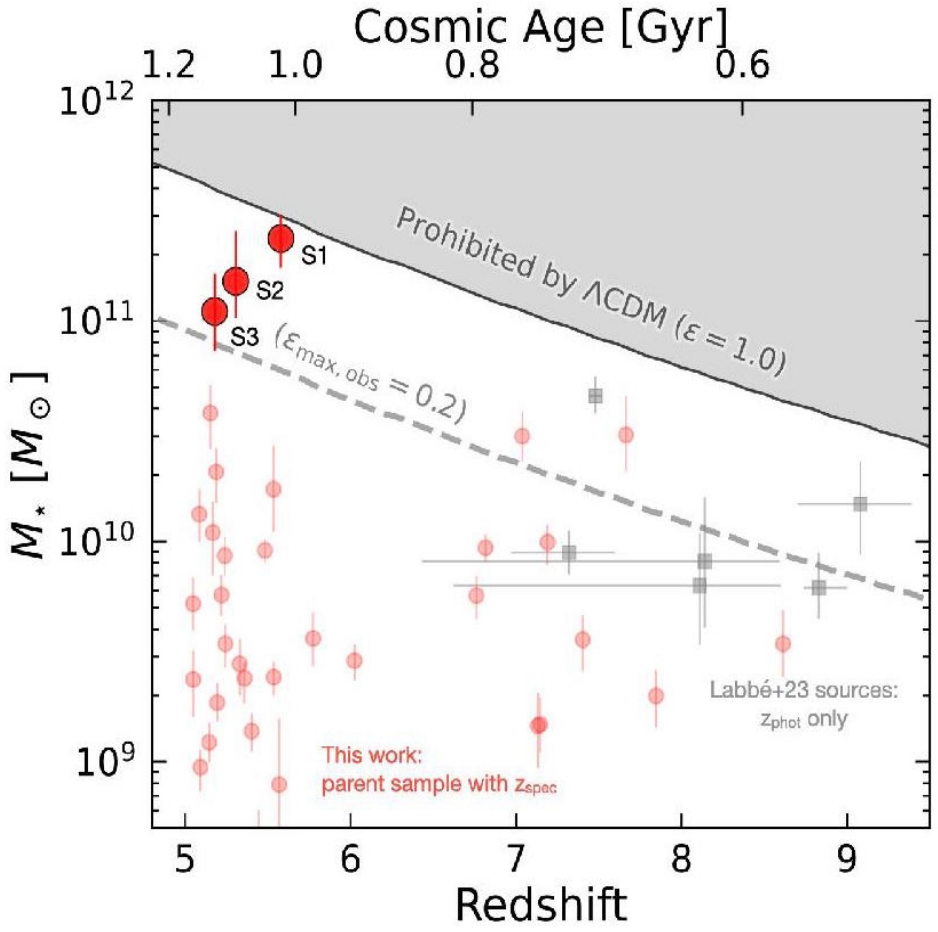

Figure 2: **Stellar masses of the three ultra-massive and optically dark galaxies (red-filled large circles) compared to model expectations.** The red-filled circles show our whole parent sample of 36 spectroscopically-confirmed optically dark/faint galaxies at $z_{\rm spec} > 5$. Unlike some massive sources reported in the literature[5] that have only $z_{\rm phot}$ (grey points), our galaxies from the JWST FRESCO survey have $z_{\rm spec}$, as well as line-corrected photometry, and thus more robust $M_\star$. The grey-shaded region indicates the stellar mass prohibited by the standard ΛCDM cosmology [30], which is calculated from the maximum halo mass ($M_{\rm halo}^{\rm max}$) that can be observed in the FRESCO survey volume, based on $M_\star^{\rm max} = \epsilon f_{\rm b} M_{\rm halo}^{\rm max}$, with a cosmic baryon fraction $f_{\rm b} = \Omega_{\rm b}/\Omega_{\rm m} = 0.158$, and the maximum theoretical efficiency of converting baryons into stars, $\epsilon = 1$. The grey dashed line indicates the maximum efficiency of $\epsilon_{\rm max,obs} \sim 0.2$ from empirical modeling methods based on observational data at lower redshift[31–33]. The three most massive galaxies in our sample require significantly higher star-formation efficiencies of $\epsilon \sim 0.5$ on average.

… в 1000 раз?!

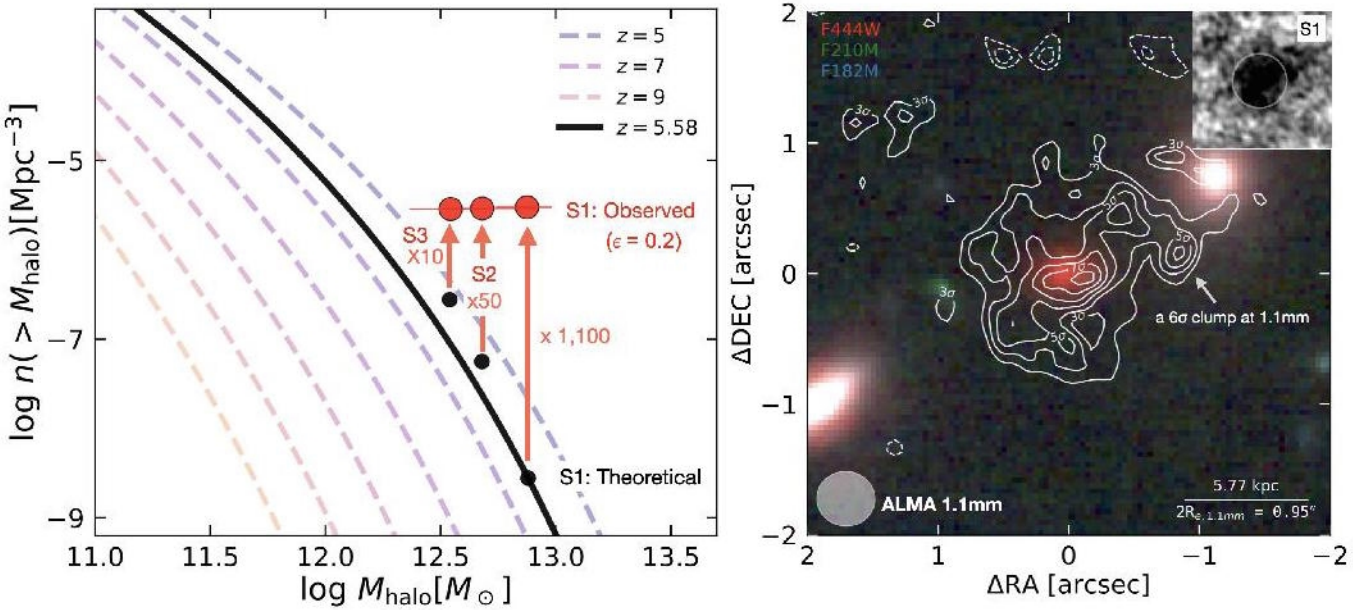

Figure 3: **The ultra-massive sources S1, S2 and S3 with $\log(M_\star/M_\odot) > 11.0$ at $z = 5-6$. Left**: Cumulative comoving number density of dark matter halos as a function of halo mass at different redshifts. We show the halo mass of S1, S2, and S3 assuming a maximum observed efficiency of $\epsilon_{\rm max,obs} = 0.2$. The observed number density derived from the FRESCO survey is shown as red points. The theoretical number density of S1, S2, and S3 in the same halo mass from the standard ΛCDM cosmology (black points) is ~1,100 times, 50 times, and 10 times lower than the observations, respectively. **Right**: The most extreme source S1 with $\log(M_\star/M_\odot) = 11.37^{+0.11}_{-0.13}$ at $z = 5.58$ exhibits an extended dust disk. We show the ALMA 1.1 mm dust contours overlaid on the JWST RGB image. The 1.1 mm image ($4'' \times 4''$) is shown in the top right corner, and the beam size ($0.''447 \times 0.''418$) is displayed in the lower left corner. The dust is clearly much more extended (half-light radius $R_e = 2.88 \pm 0.91$ kpc) compared to the stellar distribution from JWST. It also shows a 6σ clump at 1.1mm in the off-nuclear region, which, surprisingly, is undetected even in the deep, long wavelength JWST data.

Свойства необычные…

Extended Data Table 3: **Structural parameters of S1, S2, and S3.** Half light radii (R_e), sérsic indices (n), and minor over major axis ratios (q) in the F444W direct image and the grism image. Though much of the structure observed in the grism image is due to the Hα morphology, some may also be contributed by the kinematic structure and the [NII] line. The spatially extended structures and similarity of the morphologies between the grism and direct images for each object suggest that the light of these objects is not dominated by AGN.

	direct image			**Hα**		
S.No.	R_e (kpc)	n	q	R_e (kpc)	n	q
S1	0.76±0.01	1.57±0.03	0.54±0.01	0.89±0.08	0.20±0.19	0.72±0.08
S2	2.57±0.25	1.18±0.14	0.64±0.04	1.92±0.46	1.55±0.43	0.77±0.13
S3	2.22±0.09	2.31±0.09	0.42±0.01	2.10±0.09	0.20±0.11	0.18±0.02

…но это главная последовательность

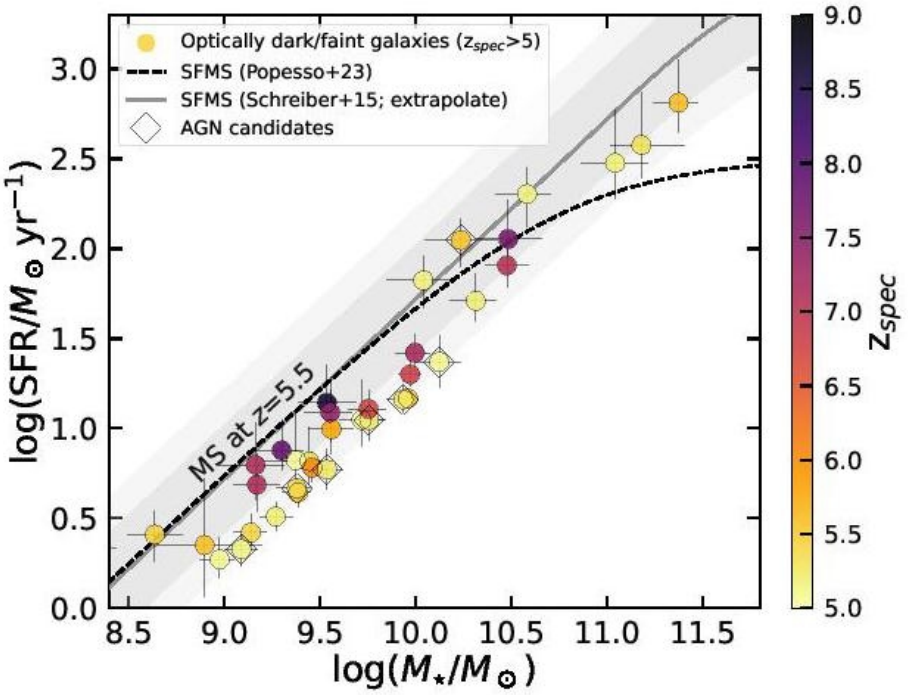

Extended Data Figure 2: **Locations of optically dark/faint galaxies compared to the SFMS in the SFR-$M_\star$ plane.** The extrapolated Schreiber SFMS[83] at z = 5.5, 1σ scatter (0.5 < ΔMS < 2, i.e., ~0.3 dex), and ±3 × ΔMS region (0.33 < ΔMS < 3, i.e., ~ 0.5 dex) are highlighted with a grey line, a dark grey shaded area, and a light grey shaded area, respectively. ΔMS > 3 is commonly used to separate MS and SB galaxies. We also plot the Popesso SFMS[84] at z = 5.5 with a dashed line.